J. Fluid Mech. (2005), *vol.* 540, *pp.* 337–351. © 2005 Cambridge University Press
doi:10.1017/S0022112005005823 Printed in the United Kingdom

On gravity–capillary lumps

By BOGUK KIM[1] AND T. R. AKYLAS[2]

[1]Department of Mathematics, Massachusetts Institute of Technology, Cambridge, MA 02139, USA

[2]Department of Mechanical Engineering, Massachusetts Institute of Technology, Cambridge, MA 02139, USA

(Received 4 October 2004 and in revised form 21 April 2005)

Two-dimensional (plane) solitary waves on the surface of water are known to bifurcate from linear sinusoidal wavetrains at specific wavenumbers $k = k_0$ where the phase speed $c(k)$ attains an extremum ($\mathrm{d}c/\mathrm{d}k|_0 = 0$) and equals the group speed. In particular, such an extremum occurs in the long-wave limit $k_0 = 0$, furnishing the familiar solitary waves of the Korteweg–de Vries (KdV) type in shallow water. In addition, when surface tension is included and the Bond number $B = T/(\rho g h^2) < 1/3$ (T is the coefficient of surface tension, ρ the fluid density, g the gravitational acceleration and h the water depth), $c(k)$ features a minimum at a finite wavenumber from which gravity–capillary solitary waves, in the form of wavepackets governed by the nonlinear Schrödinger (NLS) equation to leading order, bifurcate in water of finite or infinite depth. Here, it is pointed out that an entirely analogous scenario is valid for the bifurcation of three-dimensional solitary waves, commonly referred to as 'lumps', that are locally confined in all directions. Apart from the known lump solutions of the Kadomtsev–Petviashvili I equation for $B > 1/3$ in shallow water, gravity–capillary lumps, in the form of locally confined wavepackets, are found for $B < 1/3$ in water of finite or infinite depth; like their two-dimensional counterparts, they bifurcate at the minimum phase speed and are governed, to leading order, by an elliptic–elliptic Davey–Stewartson equation system in finite depth and an elliptic two-dimensional NLS equation in deep water. In either case, these lumps feature algebraically decaying tails owing to the induced mean flow.

1. Introduction

Two distinct kinds of solitary waves are known to exist on the surface of water, assuming two-dimensional (plane) disturbances. The first is found in shallow water and, in the weakly nonlinear limit, is governed by the celebrated Korteweg–de Vries (KdV) equation (see, for example, Whitham 1974, § 13.11); the other is possible in water of finite or infinite depth but only if surface tension is present.

The latter class of solitary waves is closely connected with the fact that the phase speed features a minimum at a finite wavenumber when both gravity and surface tension are included: as the phase speed is equal to the group speed there, this minimum is the bifurcation point of gravity–capillary solitary waves in the form of wavepackets, with crests moving at the same speed as the wave envelope (Akylas 1993; Longuet-Higgins 1993). In fact, the long-water-wave speed, at which solitary waves bifurcate in shallow water, is a local maximum (minimum) of the phase speed if the Bond number $B = T/(\rho g h^2)$ (T is the coefficient of surface tension, ρ is the fluid density, g is the gravitational acceleration and h the water depth) is less (greater)

https://doi.org/10.1017/S0022112005005823 Published online by Cambridge University Press

than 1/3; both kinds of solitary water waves thus bifurcate at extrema of the phase speed.

While solitary waves of the KdV type have been known for over a century, gravity–capillary solitary waves of the wavepacket type were discovered relatively recently. Longuet-Higgins (1989) first presented numerical evidence of gravity–capillary solitary waves in deep water, followed by a number of related analytical and computational studies (see Dias & Kharif 1999 for a comprehensive review). It turns out that two symmetric solution branches, one corresponding to elevation and the other to depression waves, bifurcate from a linear sinusoidal wavetrain at the minimum phase speed. In the small-amplitude limit, close to bifurcation, these branches are governed by the nonlinear Schrödinger (NLS) equation, their difference being merely a shift of the wave crests by half a wavelength relative to the peak of the wave envelope. In addition, there is an infinity of other symmetric and asymmetric solution branches that bifurcate at finite amplitude below the minimum phase speed; these may be interpreted as multi-packet solitary waves and are beyond the reach of the NLS equation, although they can be captured by a more refined perturbation approach (Yang & Akylas 1997).

The theory of three-dimensional solitary waves, commonly referred to as 'lumps', that are locally confined in all directions, is not as well developed. Most prior work centres around the Kadomtsev–Petviashvili (KP) equation, an extension of the KdV equation that allows for weak three-dimensional effects in the propagation of weakly nonlinear waves in shallow water. According to the KP equation, KdV solitary waves are stable (unstable) to transverse perturbations when the Bond number is less (greater) than 1/3. In the regime where instability is present, the KP equation (in which case usually called the KP-I equation) admits lump solutions with algebraically decaying tails (see, for example, Ablowitz & Segur 1979). Similar lumps were found numerically by Berger & Milewski (2000) based on the Benney–Luke equations with surface tension, a more general system of weakly nonlinear shallow-water equations than the KP-I. Like their KP-I counterparts, these lumps are possible only if the Bond number is greater than 1/3, a condition that restricts the water depth to less than a few mm, so neglecting viscous effects cannot be justified.

In the present study, it is pointed out that, when surface tension is present, lumps of the wavepacket type can be found for $B < 1/3$ in water of finite or infinite depth. In direct analogy with two-dimensional gravity–capillary solitary waves, these lumps again bifurcate at the minimum gravity–capillary phase speed and, close to bifurcation, they can be approximated as three-dimensional locally confined wavepackets with envelope moving at the same speed as the wave crests. In water of finite depth, the wave envelope and the induced mean flow are strongly coupled and are governed by an elliptic–elliptic Davey–Stewartson equation system. It turns out that the mean flow decays algebraically and so do the tails of lumps, in contrast to two-dimensional solitary waves in water of finite depth that decay exponentially at infinity. In deep water, on the other hand, the induced mean flow is relatively weak and the wave envelope is governed by an elliptic two-dimensional NLS equation to leading order; however, the induced mean flow, which again decays algebraically, prevails at the lump tails, as for two-dimensional deep-water solitary waves (Akylas, Dias & Grimshaw 1998).

While the present paper was in its final stages of preparation, we became aware of two as yet unpublished computational studies of gravity–capillary lumps, which are complementary to our weakly nonlinear analysis. Based on the full gravity–capillary water-wave equations, Parau, Vanden-Broeck & Cooker (2005) numerically

https://doi.org/10.1017/S0022112005005823 Published online by Cambridge University Press

computed two branches of symmetric elevation and depression lumps that bifurcate at the minimum phase speed; close to the bifurcation point, these lumps resemble three-dimensional wavepackets. Retaining only quadratic nonlinear terms in the governing equations, Milewski (2005) used a numerical continuation procedure to compute gravity–capillary lumps in the form of locally confined wavepackets in water of large depth, starting from shallow-water lumps of the KP-I type.

A rigorous existence proof of fully localized three-dimensional solitary-wave solutions of the gravity–capillary water-wave problem was devised by Groves & Sun (2005).

2. Expansion near the bifurcation point

Consider the classical problem of waves on the surface of water of depth h under the action of both gravity and surface tension. For the purpose of discussing waves of permanent form moving with speed c, we introduce dimensionless variables employing $T/(\rho c^2)$ as lengthscale and $T/(\rho c^3)$ as timescale, where ρ denotes the fluid density and T the coefficient of surface tension. The phase speed of linear sinusoidal gravity–capillary waves with wavenumber k is thus normalized to unity, and the dispersion relation takes the form

$$G(k;\alpha, H) \equiv k(\alpha + k^2)\tanh kH - k^2 = 0, \tag{2.1}$$

where

$$\alpha = \frac{gT}{\rho c^4}, \qquad H = \frac{h\rho c^2}{T}, \tag{2.2}$$

g being the acceleration due to gravity. This introduces two flow parameters, the speed parameter α and the inverse Weber number H; the Bond number,

$$B = \frac{T}{\rho g h^2}, \tag{2.3}$$

which is independent of the wave speed, is expressed in terms of α and H via

$$B = \frac{1}{\alpha H^2}. \tag{2.4}$$

Lumps bifurcate from linear sinusoidal waves with wavenumber $k = k_0$ corresponding to the minimum gravity–capillary phase speed and, hence, to a double root of the dispersion relation (2.1):

$$G|_0 = 0, \qquad \left.\frac{\partial G}{\partial k}\right|_0 = 0. \tag{2.5}$$

In general, for a given value of one of the two independent flow parameters, conditions (2.5) specify the wavenumber k_0 and the value of the other parameter at the bifurcation point. Here, for convenience, we treat H as a free parameter so, combining (2.1) and (2.5), k_0 and α_0 are determined from

$$k_0\tanh k_0H + \frac{k_0H}{\sinh 2k_0H} - \frac{1}{2} = 0, \tag{2.6a}$$

$$\alpha_0 = \frac{k_0}{\tanh k_0H} - k_0^2. \tag{2.6b}$$

https://doi.org/10.1017/S0022112005005823 Published online by Cambridge University Press

Equation (2.6*a*) has real roots $\pm k_0$ only if $3 \leqslant H < \infty$, and the Bond number (2.3) has to be less than 1/3 for bifurcation of lumps to be possible. In particular, $H \to 3$ corresponds to the long-wave limit

$$k_0 \to 0, \qquad \alpha_0 \to \tfrac{1}{3}, \tag{2.7}$$

while, in the deep-water limit $H \to \infty$,

$$k_0 \to \tfrac{1}{2}, \qquad \alpha_0 \to \tfrac{1}{4}. \tag{2.8}$$

In order to remain locally confined, a lump must travel at a speed less than the minimum gravity–capillary phase speed. Therefore $\alpha > \alpha_0$, and, in the neighbourhood of the bifurcation point, we write

$$\alpha = \alpha_0 + \epsilon^2, \tag{2.9}$$

ϵ being a small parameter ($0 < \epsilon \ll 1$).

Close to the bifurcation point, moreover, lumps are in the form of small-amplitude wavepackets with crests moving at the same speed (equal to 1 in the present normalization) as the wave envelope. The velocity potential $\phi(\xi, y, z)$ and the free-surface elevation $z = \eta(\xi, y)$ of a lump propagating along the x-direction (y and z denoting the transverse and vertical directions, respectively) then are expanded as follows:

$$\phi = \epsilon A_0(z, X, Y) + \epsilon\{A_1(z, X, Y)\mathrm{e}^{\mathrm{i}\theta_0} + \text{c.c.}\} + \epsilon^2\{A_2(z, X, Y)\mathrm{e}^{2\mathrm{i}\theta_0} + \text{c.c.}\} + \cdots, \tag{2.10}$$

$$\eta = \epsilon\{S_1(X, Y)\mathrm{e}^{\mathrm{i}\theta_0} + \text{c.c.}\} + \epsilon^2 S_0(X, Y) + \epsilon^2\{S_2(X, Y)\mathrm{e}^{2\mathrm{i}\theta_0} + \text{c.c.}\} + \cdots, \tag{2.11}$$

where $\xi = x - t$, $\theta_0 = k_0\xi$ and c.c. denotes the complex conjugate. The carrier wavevector $\boldsymbol{\kappa_0} = (k_0, 0)$ has magnitude $|\boldsymbol{\kappa_0}| = k_0$ as obtained from (2.6) and points in the x-direction, the crests thus being perpendicular to the propagation direction. The above expansions also assume that the amplitudes $A_0, A_1, A_2, \ldots$ and $S_0, S_1, S_2, \ldots$, which depend on the 'stretched' variables $(X, Y) = \epsilon(\xi, y)$, remain locally confined in both horizontal directions ξ and y.

The procedure for determining the amplitudes of the various harmonics in expansions (2.10) and (2.11) closely parallels that followed by Benney & Roskes (1969) and Davey & Stewartson (1974) in deriving evolution equations for three-dimensional pure-gravity wavepackets, and by Djordjevic & Redekopp (1977) and Ablowitz & Segur (1979) for gravity–capillary wavepackets.

Briefly, upon substituting (2.10) into Laplace's equation for ϕ,

$$\phi_{\xi\xi} + \phi_{yy} + \phi_{zz} = 0 \qquad (-H < z < \eta), \tag{2.12}$$

and imposing the bottom boundary condition

$$\phi_z = 0 \qquad (z = -H), \tag{2.13}$$

it follows that

$$A_1 = a_1 \frac{\cosh k_0(z+H)}{\cosh k_0 H} - \epsilon\left\{\mathrm{i}\frac{\partial a_1}{\partial X}(z+H)\frac{\sinh k_0(z+H)}{\cosh k_0 H}\right\}$$
$$- \epsilon^2\left\{\frac{1}{2}\frac{\partial^2 a_1}{\partial X^2}(z+H)^2\frac{\cosh k_0(z+H)}{\cosh k_0 H} + \frac{1}{2k_0}\frac{\partial^2 a_1}{\partial Y^2}(z+H)\frac{\sinh k_0(z+H)}{\cosh k_0 H}\right\} + \cdots, \tag{2.14a}$$

https://doi.org/10.1017/S0022112005005823 Published online by Cambridge University Press

$$A_0 = a_0 - \epsilon^2 \left\{ \frac{1}{2}(z+H)^2 \left(\frac{\partial^2 a_0}{\partial X^2} + \frac{\partial^2 a_0}{\partial Y^2} \right) \right\} + \cdots, \tag{2.14b}$$

$$A_2 = a_2 \frac{\cosh 2k_0(z+H)}{\cosh 2k_0 H} + \cdots. \tag{2.14c}$$

The next task is to satisfy the free-surface boundary conditions

$$\phi_z + \eta_\xi = \phi_\xi \eta_\xi + \phi_y \eta_y \qquad (z = \eta), \tag{2.15}$$

$$\alpha\eta - \phi_\xi + \tfrac{1}{2}\left(\phi_\xi^2 + \phi_y^2 + \phi_z^2\right) = \frac{\eta_{\xi\xi}\left(1+\eta_y^2\right) + \eta_{yy}\left(1+\eta_\xi^2\right) - 2\eta_{\xi y}\eta_\xi \eta_y}{\left(1+\eta_\xi^2+\eta_y^2\right)^{3/2}} \qquad (z=\eta). \tag{2.16}$$

Substituting expansions (2.10) and (2.11) in (2.15) and (2.16), making use of (2.14), and collecting mean terms, correct to $O(\epsilon^3)$, yields

$$-\frac{\partial S_0}{\partial X} + H\left(\frac{\partial^2 a_0}{\partial X^2} + \frac{\partial^2 a_0}{\partial Y^2} \right) + 2\left(\alpha_0 + k_0^2\right) \frac{\partial}{\partial X} |S_1|^2 = 0, \tag{2.17a}$$

$$\alpha_0 S_0 - \frac{\partial a_0}{\partial X} + \left(\left(\alpha_0 + k_0^2\right)^2 - k_0^2 \right) |S_1|^2 = 0. \tag{2.17b}$$

Eliminating S_0 from equations (2.17), it follows that $a_0(X, Y)$ satisfies

$$Q^2 \frac{\partial^2 a_0}{\partial X^2} + \frac{\partial^2 a_0}{\partial Y^2} = \lambda \frac{\partial}{\partial X} |S_1|^2, \tag{2.18}$$

where

$$\lambda = \frac{k_0^2 - \left(\alpha_0 + k_0^2\right)\left(3\alpha_0 + k_0^2\right)}{\alpha_0 H}, \qquad Q^2 = \frac{\alpha_0 H - 1}{\alpha_0 H}. \tag{2.19}$$

According to (2.2), $\alpha_0 H = gh/c_0^2$, $(gh)^{1/2}$ being the long-wave speed and c_0 the minimum gravity–capillary phase speed; hence $\alpha_0 H > 1$, and equation (2.18), which governs the $O(\epsilon^2)$ mean-flow component induced by the modulations of the packet, is of the elliptic type. As it turns out, this mean flow controls the behaviour of the tails of a lump (see § 3).

By a similar procedure, substituting the expansions (2.10) and (2.11), along with (2.14), in the free-surface conditions (2.15) and (2.16), and collecting second-harmonic terms, one finds that a_2 and S_2 satisfy

$$S_2 - \mathrm{i} \tanh 2k_0 H \; a_2 = \left(\alpha_0 + k_0^2\right) S_1^2, \tag{2.20a}$$

$$\left(\alpha_0 + 4k_0^2\right) S_2 - 2\mathrm{i}k_0 a_2 = \tfrac{1}{2}\left(3k_0^2 - \left(\alpha_0 + k_0^2\right)^2\right) S_1^2. \tag{2.20b}$$

This equation system can be readily solved for a_2 and S_2 in terms of S_1^2.

Finally, by collecting primary-harmonic terms in the free-surface conditions (2.15) and (2.16), and consistently eliminating a_2, S_2 and a_1 correct to $O(\epsilon^3)$, one may derive an amplitude equation for $S_1(X, Y)$. In view of conditions (2.5) at the bifurcation point, all $O(\epsilon)$ and $O(\epsilon^2)$ terms cancel out, and the resulting equation takes the form

$$-S_1 + \beta \frac{\partial^2 S_1}{\partial X^2} + \gamma \frac{\partial^2 S_1}{\partial Y^2} = \delta |S_1|^2 S_1 + \zeta \frac{\partial a_0}{\partial X} S_1, \tag{2.21}$$

where β, γ, δ and ζ are certain real coefficients. The equation system (2.18) and (2.21) for the primary-harmonic envelope and the induced mean flow is a steady version of the so-called Davey–Stewartson equations, derived in Davey & Stewartson (1974) following Benney & Roskes (1969).

https://doi.org/10.1017/S0022112005005823 Published online by Cambridge University Press

Obtaining expressions for the coefficients in equation (2.21), especially those multiplying the nonlinear terms, involves a considerable amount of algebra. Here, in the interest of brevity, the coefficients β and γ of the linear terms on the left-hand side of (2.21) are deduced from the linear dispersion relation, making use of the fact that a lump comprises plane waves $\boldsymbol{\kappa} = (k, m)$ that are steady in the reference frame of the lump. Hence,

$$D(k, m; \alpha) \equiv \kappa(\alpha + \kappa^2)\tanh \kappa H - k^2 = 0, \tag{2.22}$$

where $\kappa = |\boldsymbol{\kappa}|$ and, at the carrier wavevector $\boldsymbol{\kappa_0} = (k_0, 0)$,

$$D|_0 = 0, \qquad \left.\frac{\partial D}{\partial k}\right|_0 = \left.\frac{\partial D}{\partial m}\right|_0 = 0, \tag{2.23}$$

in view of (2.5). Expanding (2.22) in the vicinity of the bifurcation point,

$$\alpha = \alpha_0 + \epsilon^2, \qquad k = k_0 + \epsilon\,\Delta k, \qquad m = \epsilon\,\Delta m,$$

the $O(1)$ and $O(\epsilon)$ terms vanish by (2.23) so, correct to $O(\epsilon^2)$,

$$\left.\frac{\partial D}{\partial \alpha}\right|_0 + \frac{1}{2}\left.\frac{\partial^2 D}{\partial k^2}\right|_0 \Delta k^2 + \frac{1}{2}\left.\frac{\partial^2 D}{\partial m^2}\right|_0 \Delta m^2 = 0. \tag{2.24}$$

Equation (2.24) is entirely equivalent to the left-hand side of (2.21) if one substitutes $S_1 \propto \exp\{\mathrm{i}(\Delta k\, X + \Delta m\, Y)\}$, so

$$\beta = \frac{\frac{1}{2}\left.\dfrac{\partial^2 D}{\partial k^2}\right|_0}{\left.\dfrac{\partial D}{\partial \alpha}\right|_0} = \frac{\alpha_0 + k_0^2}{k_0}\left.\frac{\partial^2 \omega}{\partial k^2}\right|_0, \quad \gamma = \frac{\frac{1}{2}\left.\dfrac{\partial^2 D}{\partial m^2}\right|_0}{\left.\dfrac{\partial D}{\partial \alpha}\right|_0} = \frac{\alpha_0 + k_0^2}{k_0}\left.\frac{\partial^2 \omega}{\partial m^2}\right|_0, \tag{2.25}$$

where

$$\omega(\kappa) = \{\kappa(\alpha + \kappa^2)\tanh \kappa H\}^{1/2}.$$

The coefficients δ and ζ of the nonlinear terms on the right-hand side of (2.21) now can be read off from Djordjevic & Redekopp (1977) or Ablowitz & Segur (1979). After converting to the non-dimensional variables used here, evaluating these coefficients at the minimum gravity–capillary phase speed yields

$$\delta = \frac{1}{2}(\alpha_0 + k_0^2)^3 \left\{ \frac{(1-\sigma^2)(9-\sigma^2)\alpha_0 + k_0^2(3-\sigma^2)(7-\sigma^2)}{\alpha_0\sigma^2 - k_0^2(3-\sigma^2)} + 8\sigma^2 - \frac{2}{\alpha_0}(1-\sigma^2)^2(\alpha_0 + k_0^2) - \frac{3k_0^2\sigma^2}{\alpha_0 + k_0^2} \right\}, \tag{2.26a}$$

$$\zeta = 2(\alpha_0 + k_0^2)\left\{1 + \frac{(\alpha_0 + k_0^2)^2 - k_0^2}{2\alpha_0(\alpha_0 + k_0^2)}\right\}, \tag{2.26b}$$

where

$$\sigma^2 = \tanh^2 k_0 H = k_0^2/(\alpha_0 + k_0^2)^2.$$

It is easy to check that the coefficient $\gamma > 0$ and, as noted by Dias & Haragus-Courcelle (2000), $\beta > 0$ as well. Equations (2.18) and (2.21), which govern the primary-harmonic envelope and the induced mean flow, therefore, are both of the elliptic type. In this instance, as remarked by Ablowitz & Segur (1979), the Davey–Stewartson equations are not integrable by inverse scattering transforms.

https://doi.org/10.1017/S0022112005005823 Published online by Cambridge University Press

In the special case that transverse modulations are absent ($\partial/\partial Y = 0$), equation (2.18) can be readily solved for the induced mean flow:

$$\frac{\partial a_0}{\partial X} = \frac{\lambda}{Q^2}|S_1|^2, \tag{2.27}$$

and, upon substituting in (2.21), it is found that S_1 satisfies a steady form of the NLS equation:

$$-S_1 + \beta\frac{\partial^2 S_1}{\partial X^2} + \nu|S_1|^2 S_1 = 0, \tag{2.28}$$

where

$$\nu = -\delta + \frac{\zeta}{1-\alpha_0 H}\left\{k_0^2 - \left(\alpha_0 + k_0^2\right)\left(3\alpha_0 + k_0^2\right)\right\}. \tag{2.29}$$

It turns out that $\nu > 0$ so (2.28) admits the envelope-soliton solution

$$S_1 = \left(\frac{2}{\nu}\right)^{1/2} \operatorname{sech}\left\{\frac{X}{\beta^{1/2}}\right\}, \tag{2.30}$$

which, combined with (2.9) and (2.11), furnishes the well-known two-dimensional solution branches of solitary waves of elevation (+) and depression (–):

$$\eta = \pm\eta_0 \operatorname{sech}\left\{\left(\frac{\alpha-\alpha_0}{\beta}\right)^{1/2}(x-t)\right\}\cos k_0(x-t) + \cdots, \tag{2.31}$$

where, to leading order in $\alpha - \alpha_0$, the peak amplitude η_0 is given by

$$\eta_0 = 2\left(\frac{2}{\nu}\right)^{1/2}(\alpha-\alpha_0)^{1/2} + \cdots. \tag{2.32}$$

In the deep-water limit $H \to \infty$, in particular, making use of (2.8) and (2.26*a*), (2.29) yields $\nu \to 11/32$ so, according to (2.32), the peak amplitude of the bifurcating solitary-wave solutions is given by

$$\eta_0 = \frac{16}{(11)^{1/2}}(\alpha-\alpha_0)^{1/2} + \cdots, \tag{2.33}$$

consistent with earlier studies (Dias & Iooss 1993; Akylas 1993; Longuet-Higgins 1993).

When both X- and Y-modulations are present, the primary-harmonic envelope and the induced mean flow are coupled, and no analytical locally confined solutions of equations (2.18) and (2.21) are known. Nevertheless, as discussed in § 4, it is possible to compute such solutions numerically and thereby determine the branches of lumps bifurcating at $\alpha = \alpha_0$.

3. Behaviour at the tails of a lump

According to (2.30), when no transverse modulations are present, the wave envelope decays exponentially and so does the induced mean flow (2.27). In water of finite depth, therefore, two-dimensional gravity–capillary solitary wavepackets feature oscillatory tails with exponentially decaying amplitude; only in deep water, where the induced mean flow decays algebraically, are these tails algebraic (Akylas *et al.* 1998). The tails of lumps behave quite differently, however, because the induced mean flow turns out to decay algebraically at infinity, irrespective of the water depth.

https://doi.org/10.1017/S0022112005005823 Published online by Cambridge University Press

Specifically, returning to the elliptic mean-flow equation (2.18), taking the Fourier transform in X and Y yields

$$\frac{\partial a_0}{\partial X} = \lambda \int_{-\infty}^{\infty}\int_{-\infty}^{\infty} l^2 \mathscr{F}\{|S_1|^2\} \frac{\exp\{\mathrm{i}(lX+mY)\}}{Q^2l^2+m^2}\,\mathrm{d}l\,\mathrm{d}m, \tag{3.1}$$

$\mathscr{F}\{|S_1|^2\}$ being the Fourier transform of $|S_1|^2$:

$$\mathscr{F}\{|S_1|^2\} = \frac{1}{4\pi^2}\int_{-\infty}^{\infty}\int_{-\infty}^{\infty} |S_1|^2 \exp\{-\mathrm{i}(lX+mY)\}\,\mathrm{d}X\,\mathrm{d}Y.$$

Therefore, in the far field $X^2+Y^2\to\infty$,

$$\frac{\partial a_0}{\partial X} \sim \frac{\lambda}{4\pi^2} I_0 \int_{-\infty}^{\infty}\int_{-\infty}^{\infty} l^2 \frac{\exp\{\mathrm{i}(lX+mY)\}}{Q^2l^2+m^2}\,\mathrm{d}l\,\mathrm{d}m, \tag{3.2}$$

where

$$I_0 = \int_{-\infty}^{\infty}\int_{-\infty}^{\infty} |S_1|^2\,\mathrm{d}X\,\mathrm{d}Y,$$

and, upon evaluating the double integral in (3.2),

$$\frac{\partial a_0}{\partial X} \sim -\frac{\lambda}{2\pi}\frac{I_0}{Q}\frac{\partial}{\partial Y}\left\{\frac{Y}{X^2+Q^2Y^2}\right\}. \tag{3.3}$$

This confirms that the induced mean flow decays algebraically at infinity and, as a result, controls the behaviour at the tails of a lump; the envelope S_1 of the primary harmonic (as well as the higher-harmonic envelopes) decays exponentially there according to the elliptic equation (2.21), and is thus overwhelmed by the mean-flow component.

For the same reason, the free-surface elevation at the tails of a lump is dominated by the mean flow,

$$\eta \sim \frac{\epsilon^2}{\alpha_0}\frac{\partial a_0}{\partial X} \qquad (X^2+Y^2\to\infty), \tag{3.4}$$

and decays algebraically as well:

$$\eta \sim -\frac{\epsilon^2}{2\pi}\frac{\lambda}{\alpha_0}\frac{I_0}{Q}\frac{\partial}{\partial Y}\left\{\frac{Y}{X^2+Q^2Y^2}\right\}. \tag{3.5}$$

4. Lump solutions

As already remarked, no analytical locally confined solution of equations (2.18) and (2.21) is available. In the deep-water limit $H\to\infty$, where the coupling of the envelope with the induced mean flow is weak, (2.21) reduces to a steady two-dimensional NLS equation of the elliptic type, for which Strauss (1977) provided a mathematical proof that a non-trivial locally confined solution is possible. A discussion of lumps in deep water, including the effect of the induced mean flow, is deferred to § 5. Here, as suggested in Papanicolaou *et al.* (1994), this limit is used as the starting point for computing locally confined solutions of the coupled equations (2.18) and (2.21), by continuation in the parameter H.

We begin by computing locally confined solutions of (2.21) when $H\to\infty$. In this limit, it follows from (2.25) and (2.26) that

$$\beta\to 1, \quad \gamma\to 2, \quad \delta\to -\frac{11}{32}. \tag{4.1}$$

https://doi.org/10.1017/S0022112005005823 Published online by Cambridge University Press

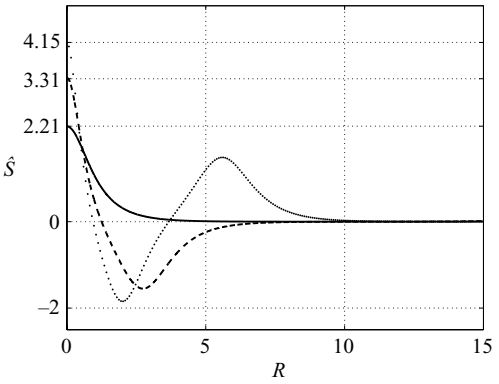


FIGURE 1. First three modes of the boundary-value problem (4.2)–(4.3) that governs localized solutions of the envelope equation (2.21) in the deep-water limit $H \to \infty$. —, ground state; - - -, second mode; $\cdots$, third mode.

Moreover, since $\lambda \to 0$ according to (2.19), the forcing term on the right-hand side of the mean-flow equation (2.18) vanishes; so $a_0 \to 0$ and, as noted above, the coupling with the induced mean flow may be neglected in equation (2.21).

With the re-scaling $\hat{Y} = Y/\sqrt{2}$ and $\hat{S}_1 = (11/32)^{1/2} S_1$, we then seek localized solutions of (2.21) which satisfy the radial NLS equation

$$\frac{\mathrm{d}^2 \hat{S}_1}{\mathrm{d}R^2} + \frac{1}{R}\frac{\mathrm{d}\hat{S}_1}{\mathrm{d}R} - \hat{S}_1 + \hat{S}_1^3 = 0, \tag{4.2}$$

where $R^2 = X^2 + \hat{Y}^2$, subject to the boundary conditions

$$\frac{\mathrm{d}\hat{S}_1}{\mathrm{d}R} = 0 \qquad (R = 0), \tag{4.3a}$$

$$\hat{S}_1 \to 0 \qquad (R \to \infty). \tag{4.3b}$$

The latter condition ensures that the disturbance remains locally confined, as required for a lump.

The boundary-value problem (4.2)–(4.3) was studied in Chiao, Garmire & Townes (1964), who found numerically a profile $\hat{S}_1(R)$ that decays monotonically in $0 < R < \infty$. Apart from this 'ground state', we also computed other, oscillatory profiles as shown in figure 1, and it appears that there exists a countably infinite set of such modes. In the following, however, only the ground state will be considered.

Starting at large depth with the localized solution of (2.21) corresponding to the ground state of (4.2)–(4.3), solutions to the coupled system (2.18) and (2.21) at finite depth were obtained via numerical continuation by gradually decreasing H. The differential equations were discretized using a pseudospectral method in terms of Chebyshev polynomials, combined with a transformation that maps the (X, Y)-plane into a bounded rectangular domain. The resulting nonlinear algebraic equations were solved by Newton's method in one quarter of the domain, exploiting symmetry. Details of numerical implementation can be found in Kim (2005).

Figure 2 illustrates the computed profiles of the envelope $S_1(X, Y)$ and the induced mean flow $\partial a_0/\partial X$ for $H = 3.5$, $H = 5$ and $H = 25$, the latter value corresponding essentially to deep water. As expected, the induced mean flow becomes stronger as H is decreased and always prevails at infinity since it decays algebraically, while S_1

https://doi.org/10.1017/S0022112005005823 Published online by Cambridge University Press

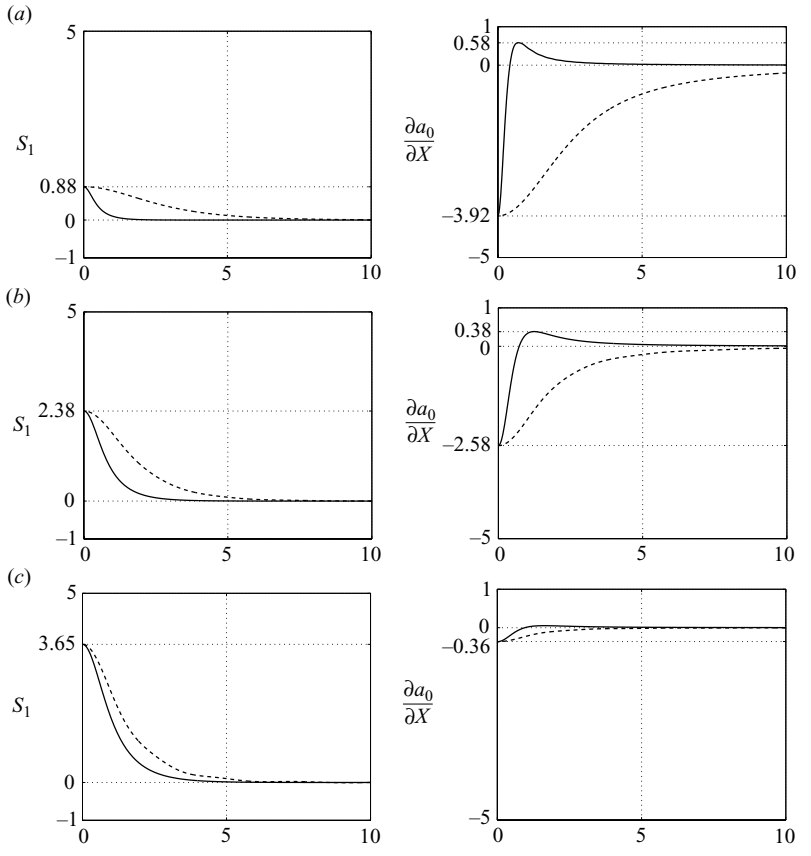


FIGURE 2. Representative profiles of the lump primary-harmonic envelope $S_1(X, Y)$ and the induced mean flow $\partial a_0/\partial X$, as obtained from the equation system (2.18) and (2.21) for various values of H. —, X-cross-section for $Y = 0$; - - -, Y-cross-section for $X = 0$. (*a*) $H = 3.5$; (*b*) $H = 5$; (*c*) $H = 25$.

decays exponentially, there. As a check of the numerical computations, it was verified that the decay of the mean flow at infinity is consistent with the asymptotic expression (3.3) derived earlier.

Figure 3 is a plot of the envelope maximum, $S_1(0, 0)$, as H is varied. For comparison, returning to (2.30), the maximum of the envelope of a two-dimensional solitary wave, $(2/v)^{1/2}$, is also shown on the same graph. It is seen that the peak amplitude of a lump, like that of a plane solitary wave, increases as H is increased. However, for a given value of H, the peak amplitude of a lump,

$$\eta_0 = 2S_1(0, 0)(\alpha - \alpha_0)^{1/2} + \cdots, \tag{4.4}$$

exceeds that of its two-dimensional counterpart, as given by (2.33), roughly by a factor of 1.5–2 depending on H.

5. Deep water

We now return to the case of deep water and discuss the bifurcation of gravity–capillary lumps in this limit. As is evident from (2.14*a*), the perturbation expansions (2.10) and (2.11) break down when $H \to \infty$ because, as it turns out, the induced mean

https://doi.org/10.1017/S0022112005005823 Published online by Cambridge University Press

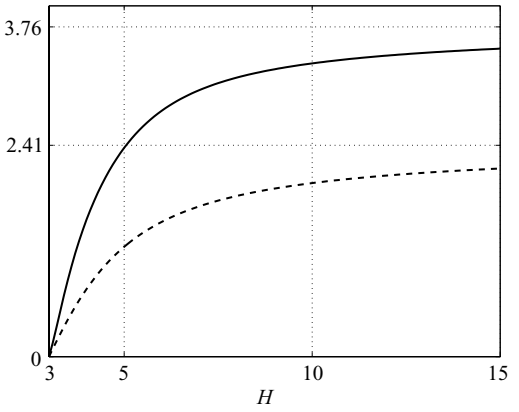


FIGURE 3. Peak amplitude of the primary-harmonic envelope S_1 as H is varied. —, three-dimensional envelope; - - -, two-dimensional envelope. The corresponding asymptotic values in the deep-water limit $H \to \infty$ are indicated by dotted lines.

flow is relatively weak, of $O(\epsilon^3)$ rather than $O(\epsilon^2)$ as assumed in (2.10) and (2.11). This disordering is also hinted by the fact that, as noted in §4, in the limit $H \to \infty$, the coupling of the primary harmonic with the induced mean flow vanishes according to (2.18), so $a_0 \to 0$.

The way to rectify the situation is now well known. As suggested by Roskes (1969), expansions (2.10) and (2.11) need to be modified such that the mean-flow terms enter at $O(\epsilon^3)$; furthermore, since the vertical coordinate becomes unbounded in deep water, it is necessary to introduce the additional stretched coordinate $Z = \epsilon z$, the velocity potential ϕ now being a function of both z and Z.

With these modifications, carrying out the perturbation analysis to $O(\epsilon^3)$ confirms that the primary-harmonic envelope $S_1(X, Y)$ satisfies precisely the steady two-dimensional NLS equation obtained by applying the formal limit $H \to \infty$ to equation (2.21), and the coefficients β, γ, and δ take the limiting values (4.1). To leading order, therefore, the coupling with the induced mean flow is negligible and the envelope of a deep-water lump is governed by the boundary-value problem (4.1)–(4.3) discussed earlier. Based on the ground state plotted in figure 1, the peak amplitude of a lump in deep water, to leading order in $\alpha - \alpha_0$, is given by (4.4) with $S_1(0, 0) = 3.76$; this is the three-dimensional counterpart of the well-known expression (2.33) for two-dimensional solitary waves in deep water.

Although the effect of the induced mean flow in deep water is of higher order, the behaviour of the tails of a lump is controlled by the mean flow. As explained in Akylas *et al.* (1998) for two-dimensional solitary waves in deep water, where a similar non-uniformity arises, the reason is that the wave envelope decays exponentially at infinity while the mean flow does so algebraically and eventually dominates at the tails. Accordingly, in order to discuss the behaviour at the tails of a lump in deep water, it is necessary to carry the perturbation analysis to $O(\epsilon^4)$.

Hogan (1985) derived a fourth-order envelope equation for three-dimensional modulations of gravity–capillary wavepackets in deep water, and we shall adapt his analysis to the case of lumps. Allowing for the fact that the carrier oscillations and the envelope move with speed 1 in the non-dimensional variables used here, and evaluating the coefficients of his evolution equation at the bifurcation point, it is

https://doi.org/10.1017/S0022112005005823 Published online by Cambridge University Press

found that the primary-harmonic envelope $S_1(X, Y)$ is governed by

$$-S_1+\frac{\partial^2 S_1}{\partial X^2}+2\frac{\partial^2 S_1}{\partial Y^2}+\frac{11}{32}|S_1|^2 S_1+\mathrm{i}\epsilon\left\{2\frac{\partial^3 S_1}{\partial X\partial Y^2}+\frac{3}{4}|S_1|^2\frac{\partial S_1}{\partial X}\right\}-\epsilon S_1\frac{\partial\bar{\phi}}{\partial X}\Big|_{Z=0}=0, \tag{5.1}$$

while the mean-flow potential $\epsilon^2\bar{\phi}(X, Y, Z)$ (that replaces $\epsilon A_0(z, X, Y)$ in (2.10)) satisfies Laplace's equation

$$\bar{\phi}_{XX}+\bar{\phi}_{YY}+\bar{\phi}_{ZZ}=0 \qquad (0>Z>-\infty), \tag{5.2}$$

subject to the boundary conditions

$$\bar{\phi}_Z=\frac{\partial}{\partial X}|S_1|^2 \qquad (Z=0), \tag{5.3a}$$

$$\bar{\phi}\to 0 \qquad (Z\to-\infty). \tag{5.3b}$$

To leading order, as expected, S_1 satisfies the elliptic two-dimensional NLS equation that is obtained from the Davey–Stewartson system (2.18) and (2.21) in the deep-water limit $H\to\infty$. It is easy to check that the higher-order modulation terms in (5.1) affect only the phase of S_1, resulting in $O(\epsilon^2)$ corrections to the carrier wavenumber, while the coupling with the induced mean flow produces an $O(\epsilon^2)$ correction to the wave amplitude.

The boundary-value problem (5.2)–(5.3) for the mean-flow potential $\bar{\phi}$ can be readily solved by taking the Fourier transform in X and Y, and the associated free-surface elevation $\bar{\eta}$ is given by

$$\bar{\eta}=-\frac{\epsilon^3}{\alpha_0}\int_{-\infty}^{\infty}\int_{-\infty}^{\infty} l^2\mathscr{F}\{|S_1|^2\}\frac{\exp\{\mathrm{i}(lX+mY)\}}{(l^2+m^2)^{1/2}}\,\mathrm{d}l\,\mathrm{d}m, \tag{5.4}$$

$\mathscr{F}\{|S_1|^2\}$ denoting the Fourier transform of $|S_1|^2$ as in (3.1).

Therefore, in the far field $X^2+Y^2\to\infty$,

$$\bar{\eta}\sim\frac{\epsilon^3}{4\pi^2\alpha_0}I_0\frac{\partial^2}{\partial X^2}\int_{-\infty}^{\infty}\int_{-\infty}^{\infty}\frac{\exp\{\mathrm{i}(lX+mY)\}}{(l^2+m^2)^{1/2}}\,\mathrm{d}l\,\mathrm{d}m, \tag{5.5}$$

where I_0 is defined as in (3.2). Upon evaluating the double integral in (5.5) and recalling that $\alpha_0=1/4$ in deep water, it is finally found that

$$\bar{\eta}\sim\frac{2\epsilon^3}{\pi}I_0\frac{\partial^2}{\partial X^2}\left\{\frac{1}{(X^2+Y^2)^{1/2}}\right\}. \tag{5.6}$$

Comparing (5.6) with the analogous expression (3.5) in water of finite depth, it is seen that the mean flow accompanying a lump in deep water is weaker and decays faster than its finite-depth counterpart. Nevertheless, since $\bar{\eta}$ decays algebraically, it eventually prevails at the tails of a lump.

6. Discussion

Based on small-amplitude expansions, we have pointed out that gravity–capillary lumps are possible for $B<1/3$ on water of finite or infinite depth. Like two-dimensional gravity–capillary solitary waves, these lumps bifurcate at the minimum gravity–capillary phase speed and, in the small-amplitude limit, close to the bifurcation point, take the form of fully localized wavepackets with envelope and crests moving at the same speed, slightly below the minimum gravity–capillary phase speed. Moreover, two symmetric lump-solution branches, one corresponding to elevation and the other

https://doi.org/10.1017/S0022112005005823 Published online by Cambridge University Press

to depression waves, bifurcate from infinitesimal sinusoidal wavetrains, as is the case of two-dimensional solitary waves. The only essential difference of lumps from their two-dimensional counterparts is that the induced mean flow always decays algebraically at infinity and so do the tails of lumps, irrespective of the water depth. This is in contrast to the tails of two-dimensional solitary waves which decay algebraically only in deep water.

Since gravity–capillary lumps travel at speeds less than the minimum phase speed, there is no possiblility of resonance with other parts of the water-wave spectrum, precluding the formation of small-amplitude oscillations at infinity, similar to those found at the tails of KdV solitary waves when the Bond number is less than $1/3$. This is consistent with the recent numerical work of Parau *et al.* (2005), who computed locally confined gravity–capillary lumps based on the full water-wave equations, and the rigorous existence proof of Groves & Sun (2005).

It is known that the bifurcation diagram of two-dimensional gravity–capillary solitary waves is quite complicated, as, in addition to the two symmetric solution branches that bifurcate at zero amplitude, there is an infinity of other, symmetric and asymmetric, branches that bifurcate at finite amplitude (see, for example, Champneys & Toland 1993). It is likely that analogous lump-solution branches could be found but, in order to capture these branches, the asymptotic approach taken here must be refined to account for exponentially small terms, as was done in Yang & Akylas (1997) for two-dimensional solitary waves.

From a physical standpoint, however, a more important question, that remains open, concerns the stability of the lumps found here. While, in analogy with the stability properties of two-dimensional solitary waves (Calvo & Akylas 2002), one might expect, close to the bifurcation point, the depression lump-solution branch to be stable and the elevation branch to be unstable, there is a property of three-dimensional wavepackets that has no counterpart in two dimensions: the elliptic–elliptic Davey–Stewartson equations, which govern the evolution of the wavepacket envelope and the induced mean flow in the small-amplitude limit, predict the formation of a focusing singularity in finite time, if the initial amplitude is above a certain threshold, the lump solution being at the borderline between stability and instability (Ablowitz & Segur 1979; Papanicolaou *et al.* 1994). The role that this type of nonlinear modulational instability may play in the propagation of lumps is not known. On the other hand, lumps resemble wavepackets in the small-amplitude limit only, so the focusing singularity of the envelope may not be relevant away from the bifurcation point.

Another related issue of physical interest is how lumps may arise from more general initial conditions. In shallow water, KP-I lumps are intimately connected with the instability of KdV solitary waves to transverse perturbations; whether a similar connection exists between gravity–capillary lumps and plane solitary waves in water of finite or infinite depth is not known, although two-dimensional gravity–capillary solitary wavepackets in fact are unstable to transverse modulations in the small-amplitude limit (Zakharov & Rubenchik 1974; Saffman & Yuen 1978).

To address the questions raised above would require solving the unsteady water-wave equations and, for this purpose, one would have to resort to fully numerical simulations.

On the other hand, we have been able to make some progress towards settling these issues in the context of a relatively simple model equation. Specifically, we studied a generalization, that allows for variations in two spatial dimensions, of the equation proposed by Benjamin (1992) for the propagation in one spatial dimension

https://doi.org/10.1017/S0022112005005823 Published online by Cambridge University Press

of long weakly nonlinear interfacial gravity–capillary waves in the strong-surface-tension regime, when both the KdV and the Benjamin–Davis–Ono (BDO) dispersive terms are equally important. In certain limits, this two-dimensional Benjamin equation admits lumps of the wavepacket type, similar to those found on water of finite depth, as well as lumps of the KP-I type. Out of the two symmetric branches of wavepacket lumps that bifurcate at the extremum of the phase speed, the elevation branch can be continued towards the KP-I lumps. Moreover, elevation lumps appear to be stable and emerge from the instability of elevation solitary waves to transverse perturbations. Detailed results will be reported in a forthcoming paper (Kim & Akylas 2005).

We wish to thank Professors Mark Ablowitz and Victor Shrira for helpful discussions. This work was supported by the Air Force Office of Scientific Research, Air Force Materials Command, USAF, under Grant Number FA9950-04-1-0125 and by the National Science Foundation Grant Number DMS-0305940.

REFERENCES

Ablowitz, M. J & Segur, H. 1979 On the evolution of packets of water waves. *J. Fluid Mech.* **92**, 691–715.

Akylas, T. R. 1993 Envelope solitons with stationary crests. *Phys. Fluids* A **5**, 789–791.

Akylas, T. R., Dias, F. & Grimshaw, R. H. J. 1998 The effect of the induced mean flow on solitary waves in deep water. *J. Fluid Mech.* **355**, 317–328.

Benjamin, T. B. 1992 A new kind of solitary wave. *J. Fluid Mech.* **245**, 401–411.

Benney, D. J. & Roskes, G. J. 1969 Wave instabilities. *Stud. Appl. Maths* **48**, 377–385.

Berger, K. M. & Milewski, P. A. 2000 The generation and evolution of lump solitary waves in surface-tension-dominated flows. *SIAM J. Appl. Maths* **61**, 731–750.

Calvo, D. C. & Akylas, T. R. 2002 Stability of steep gravity–capillary solitary waves in deep water. *J. Fluid Mech.* **452**, 123–143.

Champneys, A. R. & Toland, J. F. 1993 Bifurcation of a plethora of multi-modal homoclinic orbits for autonomous Hamiltonian systems. *Nonlinearity* **6**, 665–722.

Chiao, R. Y., Garmire, E. & Townes, C. H. 1964 Self-trapping of optical beams. *Phys. Rev. Lett.* **13**, 479–482.

Davey, A. & Stewartson, K. 1974 On three-dimensional packets of surface waves. *Proc. R. Soc. Lond.* A **338**, 101–110.

Dias, F. & Haragus-Courcelle, M. 2000 On the transition from two-dimensional to three-dimensional water waves. *Stud. Appl. Maths* **104**, 91–127.

Dias, F. & Iooss, G. 1993 Capillary–gravity solitary waves with damped oscillations. *Physica* D **65**, 399–423.

Dias, F. & Kharif, C. 1999 Nonlinear gravity and capillary–gravity waves. *Annu. Rev. Fluid Mech.* **31**, 301–346.

Djordjevic, V. D. & Redekopp, L. G. 1977 On two-dimensional packets of capillary–gravity waves. *J. Fluid Mech.* **79**, 703–714.

Groves, M. D. & Sun, S. M. 2005 Fully localised solitary-wave solutions of the three-dimensional gravity–capillary water-wave problem, preprint.

Hogan, S. J. 1985 The fourth-order evolution equation for deep-water gravity–capillary waves. *Proc. R. Soc. Lond.* A **402**, 359–372.

Kim, B. 2005 Three-dimensional solitary waves in dispersive wave systems. Doctoral dissertation, Department of Mathematics, MIT, in preparation.

Kim, B. & Akylas, T. R. 2005 On gravity–capillary lumps. Part 2. Two-dimensional Benjamin equation. *J. Fluid Mech.* (submitted).

Longuet-Higgins, M. S. 1989 Capillary–gravity waves of solitary type on deep water. *J. Fluid Mech.* **200**, 451–470.

Longuet-Higgins, M. S. 1993 Capillary–gravity waves of solitary type and envelope solitons on deep water. *J. Fluid Mech.* **252**, 703–711.

https://doi.org/10.1017/S0022112005005823 Published online by Cambridge University Press

Milewski, P. A. 2005 Three-dimensional localized solitary gravity–capillary waves. *Commun Math. Sci.* **3**, 89–99.

Papanicolaou, G. C., Sulem, G. C., Sulem, P. L. & Wang, X. P. 1994 The focusing singularity of the Davey–Stewartson equations for gravity–capillary surface waves. *Physica* D **72**, 61–68.

Parau, E., Vanden-Broeck, J.-M. & Cooker, M. J. 2005 Nonlinear three-dimensional gravity–capillary solitary waves. *J. Fluid Mech.* **536**, 99–105.

Roskes, G. J. 1969 Wave envelopes and nonlinear waves. Doctoral dissertation, Department of Mathematics, MIT.

Saffman, P. G. & Yuen, H. C. 1978 Stability of a plane soliton to infinitesimal two-dimensional perturbations. *Phys. Fluids* **21**, 1450–1451.

Strauss, W. A. 1977 Existence of solitary waves in higher dimensions. *Commun. Math. Phys.* **55**, 149–162.

Whitham, G. B. 1974 *Linear and Nonlinear Waves.* Wiley-Interscience.

Yang, T. S. & Akylas, T. R. 1997 On asymmetric gravity–capillary solitary waves. *J. Fluid Mech.* **330**, 215–232.

Zakharov, V. E. & Rubenchik, A. M. 1974 Instability of waveguides and solitons in nonlinear media. *Sov. Phys. -JETP* **38**, 494–500.

https://doi.org/10.1017/S0022112005005823 Published online by Cambridge University Press